NASA TECHNICAL NOTE

NASA TN D-5032

C. 1

NASA TN D-5032

A PARAMETRIC STUDY OF BLADE-MOTION STABILITY BOUNDARIES FOR AN ARTICULATED ROTOR

by Julian L. Jenkins, Jr.

Langley Research Center
Langley Station, Hampton, Va.

NATIONAL AERONAUTICS AND SPACE ADMINISTRATION • WASHINGTON, D. C. • FEBRUARY 1969

A PARAMETRIC STUDY OF BLADE-MOTION STABILITY BOUNDARIES FOR AN ARTICULATED ROTOR

By Julian L. Jenkins, Jr.

Langley Research Center
Langley Station, Hampton, Va.

NATIONAL AERONAUTICS AND SPACE ADMINISTRATION

For sale by the Clearinghouse for Federal Scientific and Technical Information
Springfield, Virginia 22151 – CFSTI price $3.00

A PARAMETRIC STUDY OF BLADE-MOTION STABILITY BOUNDARIES FOR AN ARTICULATED ROTOR

By Julian L. Jenkins, Jr.
Langley Research Center

SUMMARY

The blade-motion stability and response sensitivity of a fully articulated rotor (flapping and lead-lag degrees of freedom) is examined by using a numerical solution to the coupled, nonlinear, rigid-blade equations of motion. The effect of initial conditions on the tip-speed ratio for divergent motion is indicated by varying the initial azimuth angle for introducing a disturbance and by varying the disturbance amplitude at the critical azimuth angle.

Methods of extending the divergence boundary of an articulated rotor are examined. The effects of blade-root pocket cutout, hinge restraint (spring and damping), flapping-hinge cant angle, and hinge offset are evaluated individually and a representative combination of these parameters was chosen to indicate the overall effectiveness on blade-motion stability and response.

INTRODUCTION

Current efforts to extend the speed capability of rotary-wing aircraft by the addition of wings and auxiliary propulsive devices and high-speed designs which require the rotor to be stopped in flight are rapidly increasing the operating tip-speed ratios of the rotor. Tip-speed ratios in excess of 0.5 have been reached on some compound helicopters and the stopped rotor must, of course, operate through the entire range of tip-speed ratios.

Rotor operation at high tip-speed ratios increases the concern over problems of rotor stability in all the degrees of freedom and, consequently, more effort is being expended to evaluate rotor stability. Of particular concern is the blade-motion stability, since many studies have indicated that rotor-blade motion can become divergent at high tip-speed ratios. (See, for example, refs. 1 to 3.) Although reference 3 indicated the possibility of divergent blade motions, it was not intended as a comprehensive study of

the blade-motion stability problem and did not examine the methods available for extending the boundaries established.

The purpose of this report is to examine the effect on blade-motion stability of the initial conditions used to excite the motion and the effectiveness of parameters available to the designer in extending the stability limits. Also explored is the significance of the extended stability limits in terms of blade-motion response at more conventional tip-speed ratios. This study uses the programed equations of an articulated rotor blade with flapping and lagging degrees of freedom which were derived and presented in reference 4.

SYMBOLS

c blade section chord, feet (meters)

e_1 offset of center line of flapping hinge from center line of rotor shaft, feet (meters)

e_2 offset of center line of lead-lag hinge from center line of flapping hinge, feet (meters)

$e_t = e_1 + e_2$, feet (meters)

I_F equivalent mass moment of inertia of blade about flapping hinge, $\int_{e_1}^{R} m(r - e_1)^2 dr$, slug-feet^2 (kilogram-meter^2)

I_h mass moment of inertia of blade about lead-lag hinge, $\int_{e_t}^{R} m(r - e_t)^2 dr$, slug-feet^2 (kilogram-meter^2)

K_{SF} flapping spring constant, pound-foot/radian (newton-meter/radian)

K_{SL} lag spring constant, pound-foot/radian (newton-meter/radian)

m mass per unit radius, slugs/foot (kilograms/meter)

R blade radius, feet (meters)

r distance measured along blade from axis of rotation to blade element, feet (meters)

r_c radius of blade-root pocket cutout, that is, radius at which lifting surface of blade begins, feet (meters)

V velocity along flight path, feet/second (meters/second)

$x_1 = e_1/R$

$x_2 = e_2/R$

$x_c = r_c/R$

$x_t = e_t/R$

X,Y,Z orthogonal coordinate axes

α_s angle between shaft axis and plane perpendicular to flight path, positive when axis is pointing rearward, deg

β blade flapping-hinge angle with respect to shaft at particular azimuth position, radians

$\dot{\beta}$ first derivative of β with respect to time, radians/second

γ' mass constant of rotor blade, $\frac{\rho c R^4}{I_h}$

δ_3 blade flapping-hinge cant angle, degrees

ζ blade leading angle at particular azimuth position, radians

ξ ratio of added damping to critical damping

ρ mass density of air, slugs/cubic foot (kilograms/meter^3)

ψ blade azimuth angle measured from downwind position in direction of rotation, degrees

ω_n natural frequency, radians/second

Ω rotor angular velocity, radians/second

Subscripts:

F	referred to flapping hinge
L	referred to lead-lag hinge
o	initial condition
s	referred to shaft

ANALYSIS AND VARIABLES

The generalized rotor hub system is presented in figure 1. The blade is fully articulated with flapping and lead-lag degrees of freedom. The constraints on the equations of motion require that the lag hinge be coincident with or outboard of the flapping hinge. The flapping-hinge cant angle may be varied and both springs and dampers may be added to either hinge point. Blade mass factor, blade-root pocket cutout, and blade-section airfoil characteristics may also be varied. A more complete description of the hub system and equations is presented in reference 4. The analysis assumes a rigid blade, uniform inflow, and the applicability of two-dimensional airfoil characteristics.

Method of Analysis

The procedure used herein to determine stability characteristics is the same as that described in reference 4; that is, the blade was disturbed by releasing it with an initial flapping displacement β_o, at a particular azimuth position ψ_o, and the transient solution to the equations was obtained. The parameters which would produce a steady-state forced response such as blade twist, collective and cyclic pitch, and angle of attack were kept at zero so that the final response for the flapping motion would be zero for a stable condition. In other words, the solutions obtained are essentially those which would occur if an unloaded rotor were disturbed by a step increase in blade flapping angle with respect to the shaft.

The limits established are intended to indicate stability trends and do not indicate the boundary for acceptable rotor operation because of the large amplitudes which are permitted for stable cases. In this regard, the boundaries indicate motion where one or both of the angles (β or ζ) exceeded 90^o.

The procedure was to select a rotor configuration and progressively increase tip-speed ratio until the blade motion diverged when released at an azimuth angle of 90^o with a 0.2-radian initial displacement on the flapping angle β. In order to minimize the

effects of compressibility, the rotational speed of the rotor was reduced as airspeed was increased in order to maintain an advancing tip Mach number of 0.8 for all tip-speed ratios.

The parameters defining the basic rotor system are as follows:

γ'	1.6
x_c	0.2
$(\omega_n/\Omega)_F$	1.0
ξ_F	0
$(\omega_n/\Omega)_L$ $(x_t = 0.05)$	0.28
ξ_L	0
δ_3, deg	0

Variables Considered

As pointed out in reference 3, the predominant factor affecting blade-motion stability is the negative or destabilizing aerodynamic spring forces which are produced in the forward quadrants of the rotor disk ($\psi = 90^o$ to 270^o). It was shown in reference 4 that the negative aerodynamic spring moment neutralizes the centrifugal restoring moments in the forward quadrants at tip-speed ratios below 1.0 for blades with a mass constant greater than 1.0. Thus, methods of hub design which increase restoring spring forces or increase damping should delay blade-motion divergence. The parameters considered herein are not intended to include all methods for delaying divergence but do indicate the relative improvement which may be achieved without resorting to sophisticated feedback mechanisms.

The hinge restraints were added without consideration of the structural loads since this analysis is a rigid-blade analysis to establish trends and is not a design analysis. Of course, methods which involve blade-root restraint must be evaluated on the basis of detailed structural design and the improvement in stability could obviously be limited by the structural integrity of the rotor system.

The parameters considered herein are as follows:

(1) Blade mass factor

(2) Blade-root pocket cutout

(3) Flapping-hinge restraint

(4) Lead-lag-hinge restraint

(5) Flapping-hinge cant angle

(6) Hinge offset

RESULTS AND DISCUSSION

In order to avoid the large number of rotor configurations which may be established with the several parameters considered, each parameter has been considered as an independent variable when possible. Thus, with the exception of the two hinge offset distances, the parameters have been evaluated as to their effect on the divergence tip-speed ratio of a specific rotor system for specified initial conditions. The hinge points could not be changed independently in all cases since the constraints of the equations require the lagging hinge to be coincident with or inboard of the blade-root pocket cutout and the flapping hinge coincident with or inboard of the lagging hinge $\left(\text{that is, } x_1 \leqq x_t \leqq x_c\right)$.

The results are presented for the effects of the individual parameters on the divergence tip-speed ratio and then the effect of a specified combination of parameters is evaluated at more conventional tip-speed ratios.

Effect of Blade Mass Constant and Initial Conditions

The blade mass constant was used as a variable in reference 3 and boundaries were established for disturbances at two initial azimuth angles. Figure 2, which was taken from the reference, illustrates the trend of blade-motion stability with varying mass constant.

Since the mass constant γ' is inversely proportional to blade inertia (that is, high inertia produces a low mass constant), the trends illustrated indicate an improvement in blade-motion stability with increasing blade inertia.

Figure 2 also indicates a sizable increment in the tip-speed ratio for divergent motion for the two initial azimuth angles selected. In order to establish the variation in the stability boundary as the initial azimuth angle is changed, a 0.2-radian flapping-angle disturbance was introduced around the azimuth for a rotor with a mass constant of 1.6. The resulting boundary is presented in figure 3. The variation of the boundary verifies what might be expected; rotor stability is highly dependent on the location of the disturbance input and the advancing side of the disk ($\psi = 0^\circ$ to 180°) is more critical in this regard. (See ref. 4.) This condition occurs because the aerodynamic spring forces are destabilizing in the forward quadrants of the disk and are extremely strong in the second quadrant ($\psi = 90^\circ$ to 180°).

On the retreating side of the disk ($\psi = 180^\circ$ to 360°), the boundary is relatively insensitive to the location of the disturbance as indicated; however, an area below the divergence boundary produced a limit cycle motion in that the flapping motion reached a steady-state limited-amplitude response.

Since the boundary in figure 3 indicates that the region near 90° azimuth is most critical for a displacement disturbance, it is of interest to evaluate the effect of initial disturbance amplitude β_0 on the divergence boundary. This effect was evaluated in reference 4 and the resulting boundary is shown in figure 4. The results show an increase in the divergent tip-speed ratio for decreasing disturbance amplitude β_0. A comparison of figures 3 and 4 shows that a disturbance amplitude of 0.2 radian introduced on the retreating side of the disk is roughly equivalent to a 0.02-radian disturbance introduced at 90° azimuth.

The sensitivity of the boundary at $\psi_0 = 90^{\circ}$ for varying disturbance amplitudes is somewhat analogous to the change in stability which would occur for a lifting rotor. For example, if the rotor lift produced a maximum flapping angle at $\psi_0 = 90^{\circ}$ equivalent to those shown in figure 4 or if the flapping due to lift plus flapping due to a disturbance (such as a gust) produced the required angle, the rigid-blade motion would diverge.

Effect of Blade-Root Pocket Cutout

The adverse effects on performance of inboard aerodynamics of a rotor at high tip-speed ratio have been demonstrated previously. (See ref. 5.) In the same manner, blade-root pocket cutout offers a means of improving the stability characteristics by eliminating or decreasing undesirable aerodynamic forces on the inboard portion of the rotor as is illustrated in figure 5. Blade-root pocket cutout reduces both the aerodynamic spring and damping forces by an amount dependent on the blade spar and/or cuff design. The trends presented herein do not consider the root-spar aerodynamics and, consequently, are somewhat optimistic.

Although the cutout diminishes both the destabilizing spring forces and the stabilizing damping forces in the forward quadrants, the relative effects are not the same. For example, at $\psi = 180^{\circ}$, the aerodynamic spring force is a function of $V \sin \beta$, which is constant along the blade, whereas the damping force is a function of $\dot{\beta} r$ and for small values of r, very little damping force is developed. Thus, blade-root pocket cutout provides a means for reducing the aerodynamic spring forces without appreciably reducing the blade damping moment.

Effect of Flapping-Hinge Restraint

Spring restraint.- The addition of a spring restraint is equivalent in some respects to eliminating the hinge. In addition, by proper selection, hinge offset and spring restraint may be used to represent the cantilevered blade first-bending-mode shape as pointed out in reference 6.

The results obtained for the addition of a spring restraint with no hinge offset are presented in figure 6 as a function of the frequency ratio of the flapping motion which was

obtained by the following expression:

$$\left(\frac{\omega_n}{\Omega}\right)_F = \left(1 + \frac{K_{SF}}{I_F \Omega^2}\right)^{1/2}$$

The spring constant K_{SF} was adjusted to maintain a constant frequency ratio as the rotational speed was decreased.

The results indicate a near-linear increase in the divergence boundary with increasing frequency (that is, a higher spring constant). For frequency ratios from 1.0 to approximately 1.5, the blade flapping-hinge motion diverges, whereas above 1.5, the lagging motion becomes divergent. This change in the mode of divergence apparently results from the coriolis acceleration terms in the lead-lag equation of motion reaching magnitudes large enough to cause very high inplane amplitudes. As evidenced by the slight decrease in the slope of the boundary at the higher frequency ratios, the lag disturbance is apparently approaching a limiting value which causes a very rapid divergence of the lag motion. It should again be emphasized that structural considerations would limit the degree of restraint which can be incorporated into a blade design and thus the improvement achieved would depend on such considerations.

Damper restraint.- The extension in the divergence boundary for increased flapping-hinge damping is presented in figure 7. These results indicate a rapid improvement in the tip-speed ratio at which divergence occurs for up to 20 percent of critical viscous damping. Above 20 percent, the increased damping does not produce any substantial increase in the divergence tip-speed ratio. This decrease in flapping-damper effectiveness is due to the buildup in amplitude of the inplane motion until it becomes the divergent mode. Even though there is adequate damping to prevent a flapping divergence, the initial flapping response apparently produces inplane coriolis accelerations large enough to cause divergence similar to that encountered with the flapping-hinge spring restraint.

It is apparent from the results presented in this section that realization of the total benefit of either type of flapping restraint will require an inplane restraint. These restraints are investigated in the following section.

Effect of Lead-Lag-Hinge Restraint

Spring restraint.- The effect of lag-hinge spring restraint on the divergence boundary is presented in figure 8. These results are presented as a function of the frequency ratio given by the following expression:

$$\left(\frac{\omega_n}{\Omega}\right)_L = \left[\frac{3}{2}\frac{x_2}{1 - x_t}(1 + p)\right]^{1/2}$$

where

$$p = \frac{K_{SL}}{\frac{3}{2} I_h \frac{x_2}{1 - x_t} \Omega^2} = \frac{\text{Spring constant}}{\text{Centrifugal spring constant}}$$

The base point of the boundary occurs at a frequency ratio of 0.28 which corresponds to the basic inplane natural frequency for a 0.05 lag-hinge offset. As the frequency ratio is increased by increasing the lag-hinge spring constant, there is an initial improvement in the divergence boundary; however, as the frequency ratio approaches 1.0, the tip-speed ratio for convergent motion is reduced significantly. Above a frequency ratio of 1.0, the boundary again shows an improvement. At frequency ratios approaching 2.0, the blade undergoes a pure divergence in the flapping mode. This type of nonoscillatory divergence will be discussed further in the section considering lag-hinge damping restraint.

Accompanying the reduction in the divergence boundary for frequency ratios near 1.0 was an area below the boundary wherein a limit cycle motion was encountered. This area is outlined in figure 8. The blade-motion characteristic of the points used to establish this area was a steady-state, $\frac{1}{2}$-per-revolution flapping motion. Even though the expected flapping response should be of zero amplitude below the boundary, there exists an area where there is a self-excited nondivergent flapping motion which attains a steady-state amplitude. There is the possibility of other such areas existing; however, with the numerical technique used herein, it is not feasible to define them without prior knowledge of the approximate conditions required.

Damper restraint.- The results obtained for the addition of an inplane damper are presented in figure 9. The trends indicated are similar to those obtained with the addition of flapping-hinge damping (see fig. 7); however, the mode of divergence differs for the two cases. As mentioned previously, the effectiveness of the flapping-hinge damper is limited by the divergent inplane mode at damping ratios above 0.2, whereas the boundary for the lag damper results in all cases from a divergent flapping mode. In fact, above a damping ratio of 1.0, the blade-flapping motion undergoes a pure divergence (that is, nonoscillatory) when released with the specified initial conditions. This condition was also shown to be true for the lag-hinge spring restraint. (See fig. 8.) Thus, the boundaries established for either lag-hinge spring restraint or damping restraint appear to be approaching an asymtote which is in the region of the flapping divergence boundary established for a single-degree-of-freedom flapping rotor. As pointed out in reference 2, flapping instability occurs at a tip-speed ratio of 2.0 for a blade with the mass factor used herein.

Just as the effectiveness of flapping-hinge restraint was limited by lag-motion divergence, the effectiveness of lag-hinge restraint is similarly seen to be limited by flapping-motion divergence. It would appear, therefore, that a combination of both types of restraints would prove most effective in extending the divergent boundary.

Effect of Flapping-Hinge Cant Angle

Blade pitch-flap coupling represents one of the simplest feedback mechanisms which can be incorporated on a rotor, and since its function is to reduce blade loading with increasing flapping angle, it may be considered as being analogous to increasing the spring stiffness. The spring constant is nonlinear since the aerodynamic forces produced are a function of both blade azimuth position and tip-speed ratio. In addition, in the reversed velocity region the effect of positive δ_3 is reversed and produces a negative spring effect. Nevertheless, increasing the flapping-hinge cant angle provides a very effective mechanism for extending the divergence boundary for an articulated rotor as is illustrated in figure 10. The nonlinearities which exist in the boundary are apparently dependent on the mode of divergence. In all cases, both the flapping and lagging amplitudes were very large and for the δ_3 angles considered, the mode of divergence alternated between the two degrees of freedom.

A comparison of the boundary for flapping-hinge spring restraint (fig. 6) and the boundary for flapping-hinge cant angle (fig. 10) indicates that approximately 40° hinge-line cant is equivalent to doubling the frequency ratio by the addition of blade-root spring restraint.

Effect of Hinge Offset

Lag-hinge offset.- As pointed out earlier, the constraints of the equations considered require the lag hinge to be coincident with or inboard of the blade-root pocket cutout; thus, the lag hinge could only be moved outboard beyond 0.2R without introducing the additional effect of cutout. In order to consider higher values of hinge offset, it was necessary to alter the base-line cutout parameter of the rotor. Thus, two boundaries are established for increasing hinge offset. One is for the rotor system with 0.2R cutout and the second with 0.5R cutout. Both boundaries are presented in figure 11 as a function of the inplane frequency ratio as obtained from the following expression:

$$\left(\frac{\omega_n}{\Omega}\right)_L = \left(\frac{3}{2}\frac{x_2}{1 - x_t}\right)^{1/2}$$

It should be noted that the mass m was held constant from the flapping hinge out to the blade tip regardless of lag-hinge location so that the blade inertia about the flapping hinge is constant. The inertia about the lag hinge is, however, decreased.

A comparison of the boundary for lag-hinge spring restraint (fig. 8) and the lower boundary of figure 11 ($x_c = 0.2$) indicates essentially the same trend in the stability boundary for equal frequency ratios as might be expected. The upper boundary ($x_c = 0.5$) follows the same trend up to a frequency ratio $\omega_n/\Omega = 0.6$; however, the base point of the stability boundary is shifted upward as a result of the effect of increasing blade-root pocket cutout. As the frequency ratio is increased above 0.6 by increasing lag-hinge offset, the same decrease in the boundary which occurred with lag-hinge spring restraint is observed. For the conditions evaluated, however, the rotor did not exhibit the limit cycle motions that were observed for the conditions where lead-lag-hinge spring restraint was used to alter the frequency ratio.

Flapping-hinge offset.- Variations in flapping-hinge offset were accomplished within the constraints by increasing the lag-hinge offset out to 0.2R. The change in lag-hinge offset extends the base-line boundary to a tip-speed ratio of approximately 1.7 as is indicated in figure 11.

Changes in flapping-hinge offset distance also produce significant changes in the effective inertia about the flapping hinge. For example, moving the hinge offset from the center line of rotation to 0.2R reduces the flapping inertia by approximately 50 percent if the blade mass per unit length remains constant. Thus, in order to isolate the effect of changes in the stability boundary due to flapping-hinge offset, the blade mass per unit length was increased so that the effective flapping inertia remained constant. The results are presented in figure 12. Also included in the figure is the boundary which was obtained for hinge variations with a constant mass per unit length.

The boundaries are presented as a function of the flapping natural frequency ratio obtained by the following expression:

$$\left(\frac{\omega_n}{\Omega}\right)_F = \left(1 + \frac{3}{2}\frac{x_1}{1 - x_1}\right)^{1/2}$$

A comparison of the results presented in figure 6, wherein the frequency ratio was increased by spring restraint, with the results of figure 12, indicates approximately the same incremental extension in the boundary as the frequency ratio is increased. This extension is achieved, however, at the expense of increased blade weight in order to maintain the same flapping inertia. On the other hand, if the offset from 0 to 0.2R is accomplished while constant mass per unit length is maintained, there is a decrement in the boundary. The incremental decrease in tip-speed ratio, in fact, is about the same as indicated in figure 2 for the case where the blade mass constant is increased from the base-line value of 1.6 to about 3.2 (corresponding to a 50-percent reduction in flapping inertia). It would appear from these results that a minimum flapping-hinge offset would be desirable in order to obtain the maximum flapping inertia without increasing the blade weight.

Effect of Selected Combination of Parameters

In order to assess the overall effectiveness of combining methods for extending the stability boundary, a selected combination of the design parameters was evaluated and compared with the total extension which would be expected if the individual increments could be added linearly.

The rotor-hub parameters selected for this evaluation and the approximate increment achieved on an individual basis are shown in the following table:

Parameter	Value selected	$\Delta\left(\frac{V}{\Omega R}\right)$
Blade-root pocket cutout	$x_c = 0.3$	0.1
Flapping-spring restraint	$\omega_n/\Omega = 1/2$	.3
Flapping-damper restraint	$\xi = 0.2$	.5
Lag-spring restraint	$\omega_n/\Omega = 0.6$	.3
Lag-damper restraint	$\xi = 1.0$	.7
Flapping-hinge cant angle	$\delta_3 = 30^o$	1.3
Total increment		3.2

Again, the indicated frequency and damping ratios were maintained as rotational speed was reduced by adjusting the spring and damper constants. The total increment from the preceding table is $\Delta(V/\Omega R) = 3.2$. This increment plus the base-line tip-speed ratio of 1.4 indicates an extension of the divergence boundary to $V/\Omega R = 4.6$.

The combined parameters did not produce the total extension which might be anticipated on the basis of the linear combination of the individual increments. In fact, the flapping amplitude exceeded the 90^o criterion at a tip-speed ratio of approximately 4.2.

As previously mentioned, the damping and spring constants were varied in order to maintain the desired frequency and damping ratios. In practice, however, changing rotational speed in order to maintain constant tip Mach number for all tip-speed ratios will also change both the frequency ratio and the damping ratio about the two hinges. In order to show the effect of the changing frequency and damping ratios as the rotor rotational speed is reduced, the spring and damper constants were selected so that the frequency and damping ratios indicated in the preceding table are valid at a tip-speed ratio of 1.0. With the constants fixed in this manner, the tip-speed ratio was progressively increased until the blade motion became divergent.

The results are presented in figure 13 as a boundary showing the effect of initial disturbance amplitude. Also included is the boundary from figure 4 for the basic rotor without hinge restraints or δ_3. These data indicate that the constrained rotor is stable for tip-speed ratios 4 to 5 times as high as the basic rotor. This large difference in the

divergence boundaries should also be indicative of a reduction in the response sensitivity at lower tip-speed ratios.

Response Sensitivity of a Constrained Rotor

As an example of the reduction in blade-motion response which may be achieved by incorporating hub restraints, the rotor system defined in the preceding section was subjected to shaft angle-of-attack step inputs with $\psi_0 = 0^\circ$ and the maximum peak-to-peak amplitude of the ensuing motion was obtained. The results are presented in figure 14 for a tip-speed ratio of 1.0 and a tip Mach number of 0.8. The response of the rotor without restraints is also included for comparison.

The data in figure 14 indicate a sizable reduction in amplitude of the transient response for the constrained rotor as compared with the basic rotor. If, for example, 15° amplitudes represented the point at which the blade would strike the flapping stops, the basic rotor would reach this limit with very small disturbances. On the other hand, the constrained rotor does not exceed an amplitude of 10° for a 6° change in angle of attack. Since an angle-of-attack change of 6° is equivalent to a vertical gust of approximately 47 feet per second, the constrained rotor would have to be subjected to the most extreme disturbance before encountering the 15° limit. Again it should be pointed out that the restraints have been incorporated without consideration of the structural aspects, which could, of course, limit the degree of restraint which can be incorporated into a blade design.

CONCLUDING REMARKS

The blade-motion stability of a fully articulated rotor has been examined by use of a numerical solution to the coupled, nonlinear, rigid-blade equations of motion utilizing uniform inflow and two-dimensional airfoil characteristics. The results indicate that variations in the magnitude or initial azimuth of the disturbance can produce large changes in the tip-speed ratio for divergent motion.

Methods of extending the divergence boundary were also examined. Blade-root pocket cutout was shown to provide some improvement in the tip-speed ratio for divergent motion. Spring and damping restraint on either the flapping hinge or the lag hinge were also shown to be effective. These restraints, however, may be limited in effectiveness by the structural integrity of the system. Flapping-hinge cant angle proved to be most effective in delaying divergence, and from the standpoint of structural considerations, could be utilized more fully than the physical restraints such as springs and dampers.

Lag-hinge offset provided about the same improvement at comparable lag-frequency ratios as was achieved by increasing the lag-hinge spring constant. On the other hand, increasing flapping-hinge offset produced a decrement in the tip-speed ratio for divergence unless the blade mass was increased in order to maintain a constant blade inertia about the flapping hinge.

A combination of the individual restraints increased the divergence boundary to tip-speed ratios 4 to 5 times as high as the unconstrained rotor. In addition, the flapping response to vertical gusts was reduced by over 75 percent at a tip-speed ratio of 1.0 as a result of the restraints used.

Langley Research Center,
National Aeronautics and Space Administration,
Langley Station, Hampton, Va., December 11, 1968,
721-01-00-29-23.

REFERENCES

1. Horvay, Gabriel: Rotor Blade Flapping Motion. Quart. Appl. Math., vol. V, No. 2, July 1947, pp. 149-167.

2. Jenney, David S.; Arcidiacono, Peter J.; and Smith, Arthur F.: A Linearized Theory for the Estimation of Helicopter Rotor Characteristics at Advance Ratios Above 1.0. Proceedings of the Nineteenth Annual National Forum, Amer. Helicopter Soc., Inc., May 1963, pp. 38-58.

3. Jenkins, Julian L., Jr.: Calculated Blade Response at High Tip-Speed Ratios. Conference on V/STOL and STOL Aircraft. NASA SP-116, 1966, pp. 17-27.

4. Jenkins, Julian L., Jr.: A Numerical Method for Studying the Transient Blade Motions of a Rotor With Flapping and Lead-Lag Degrees of Freedom. NASA TN D-4195, 1967.

5. Gessow, Alfred; and Gustafson, F. B.: Effect of Blade Cutout on Power Required by Helicopters Operating at High Tip-Speed Ratios. NASA TN D-382, 1960.

6. Ward, John F.: Exploratory Flight Investigation and Analysis of Structural Loads Encountered by a Helicopter Hingeless Rotor System. NASA TN D-3676, 1966.

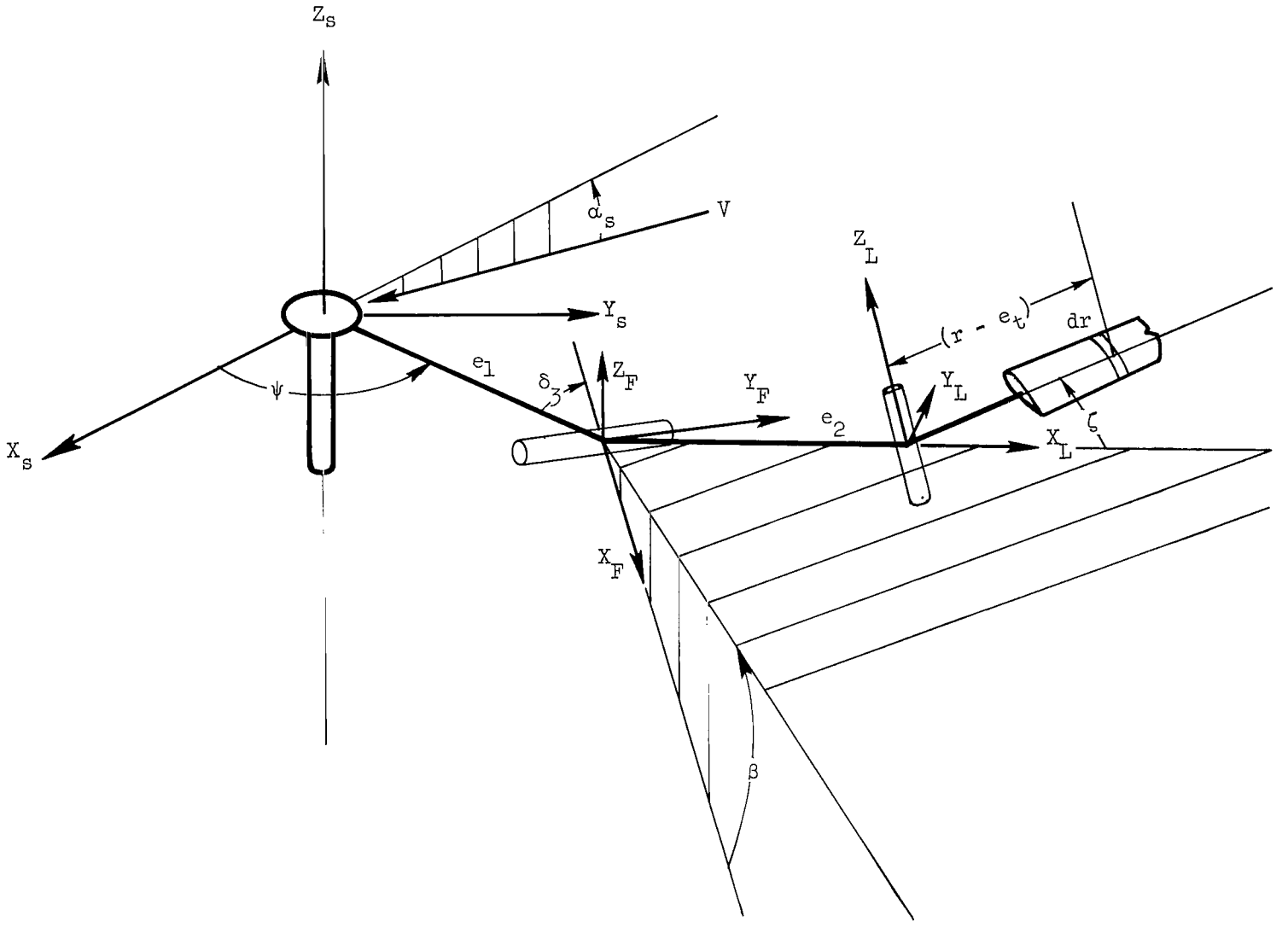

Figure 1.- Geometry of rotor hub.

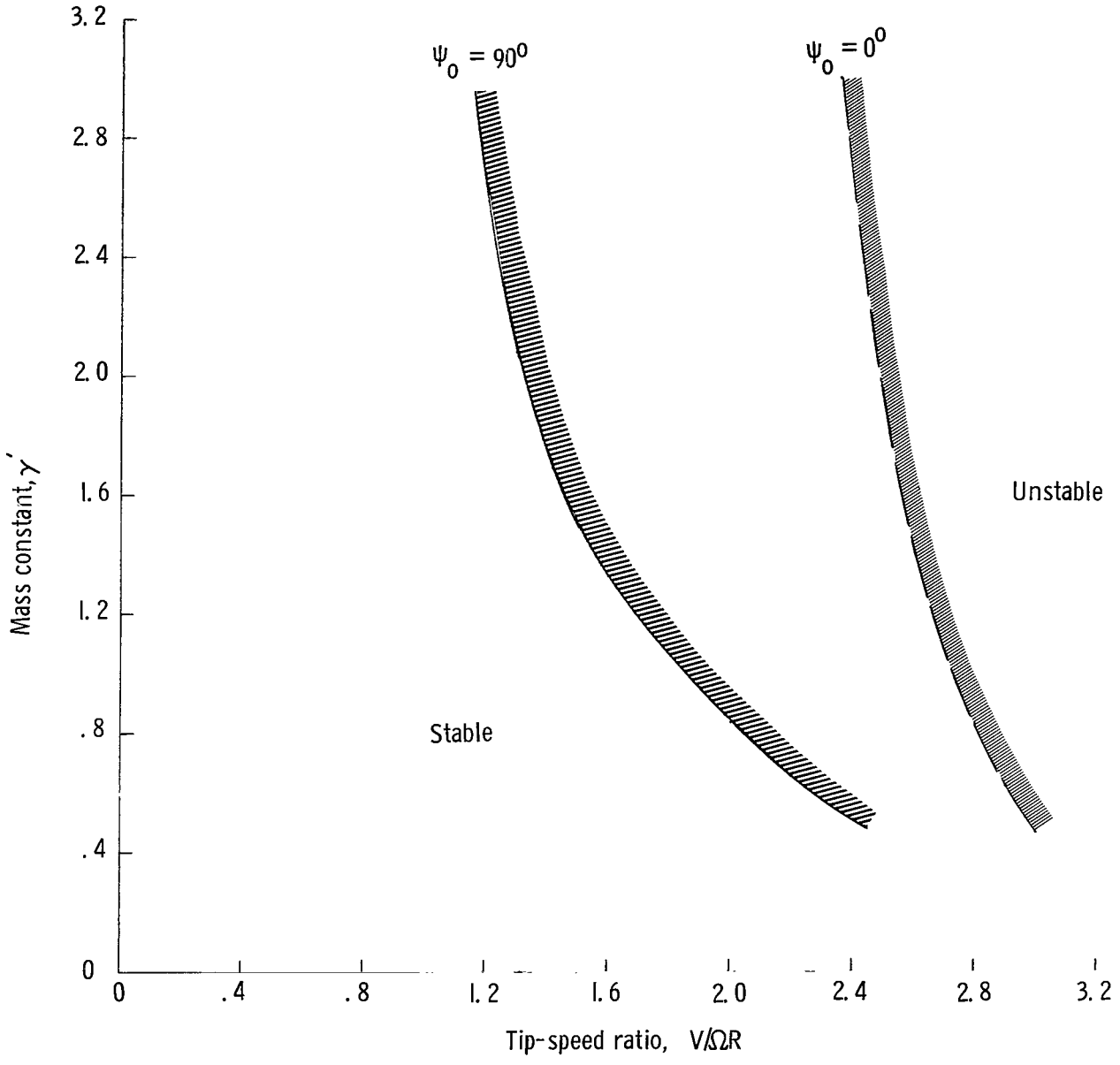

Figure 2.- Effect of blade mass constant on blade-motion stability. $\beta_0 = 0.2$ rad.

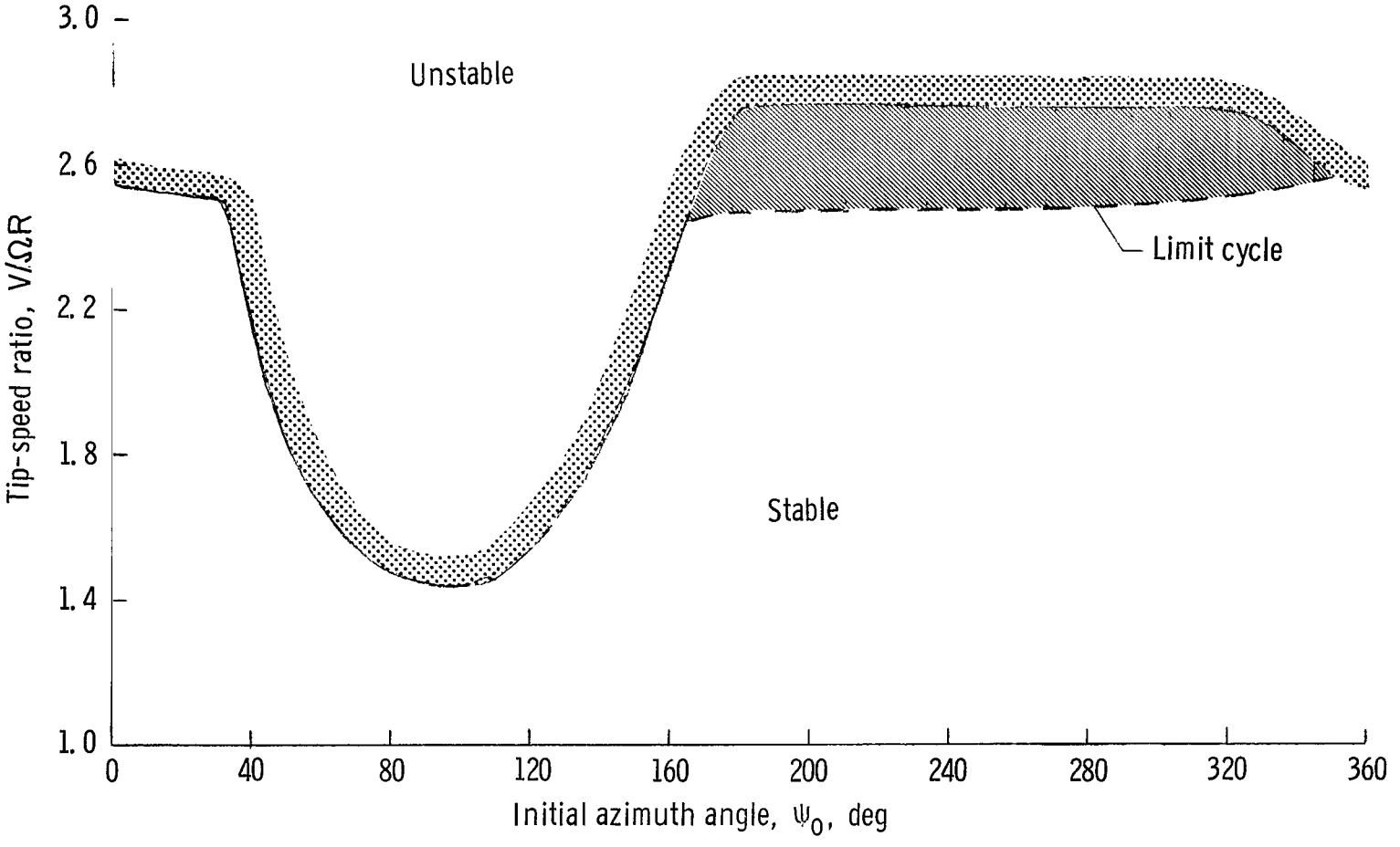

Figure 3.- Effect of initial azimuth angle on blade-motion stability. $\beta_0 = 0.2$ rad.

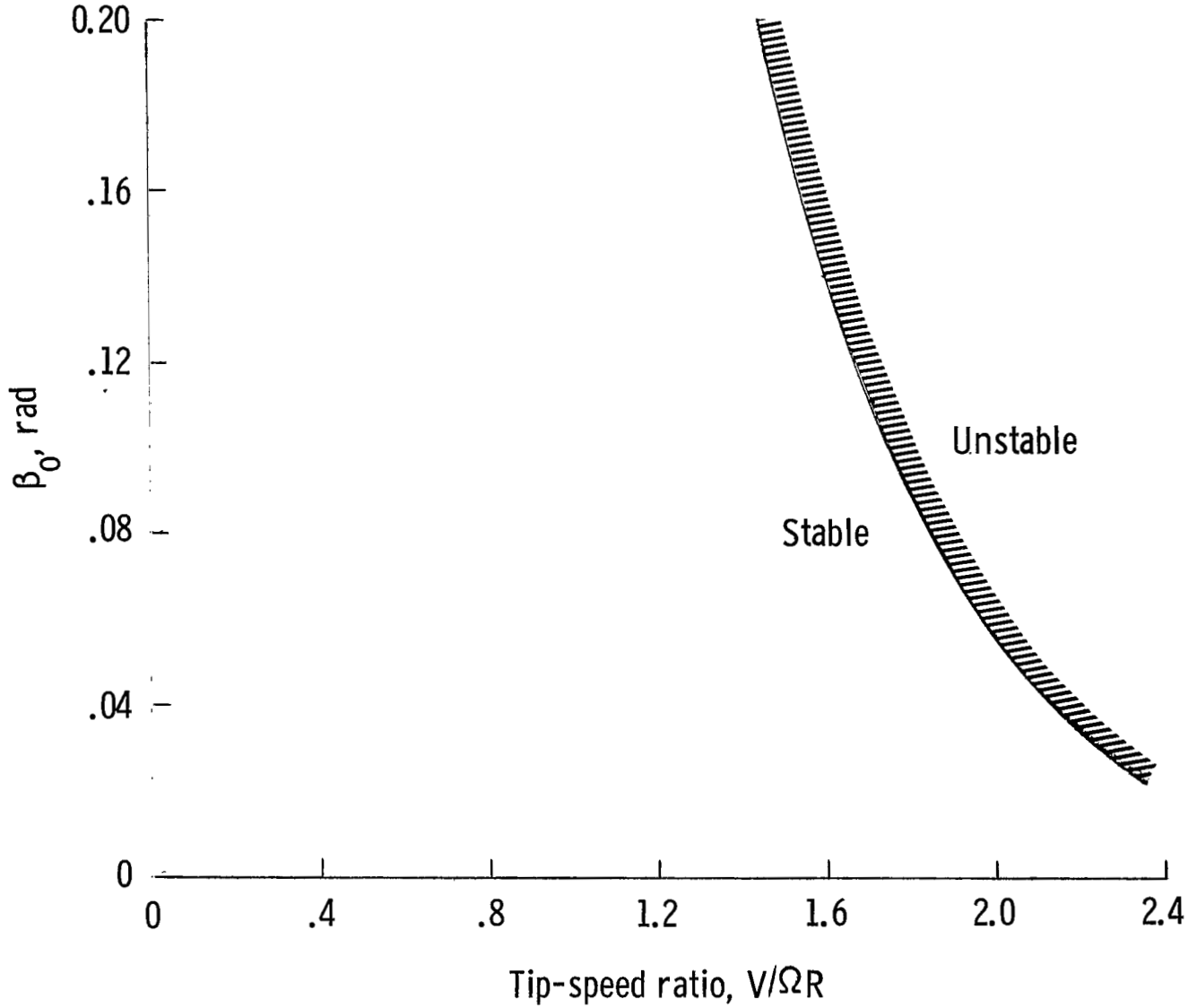

Figure 4.- Effect of initial flapping-angle displacement β_0 on blade-motion stability. $\psi_0 = 90^0$.

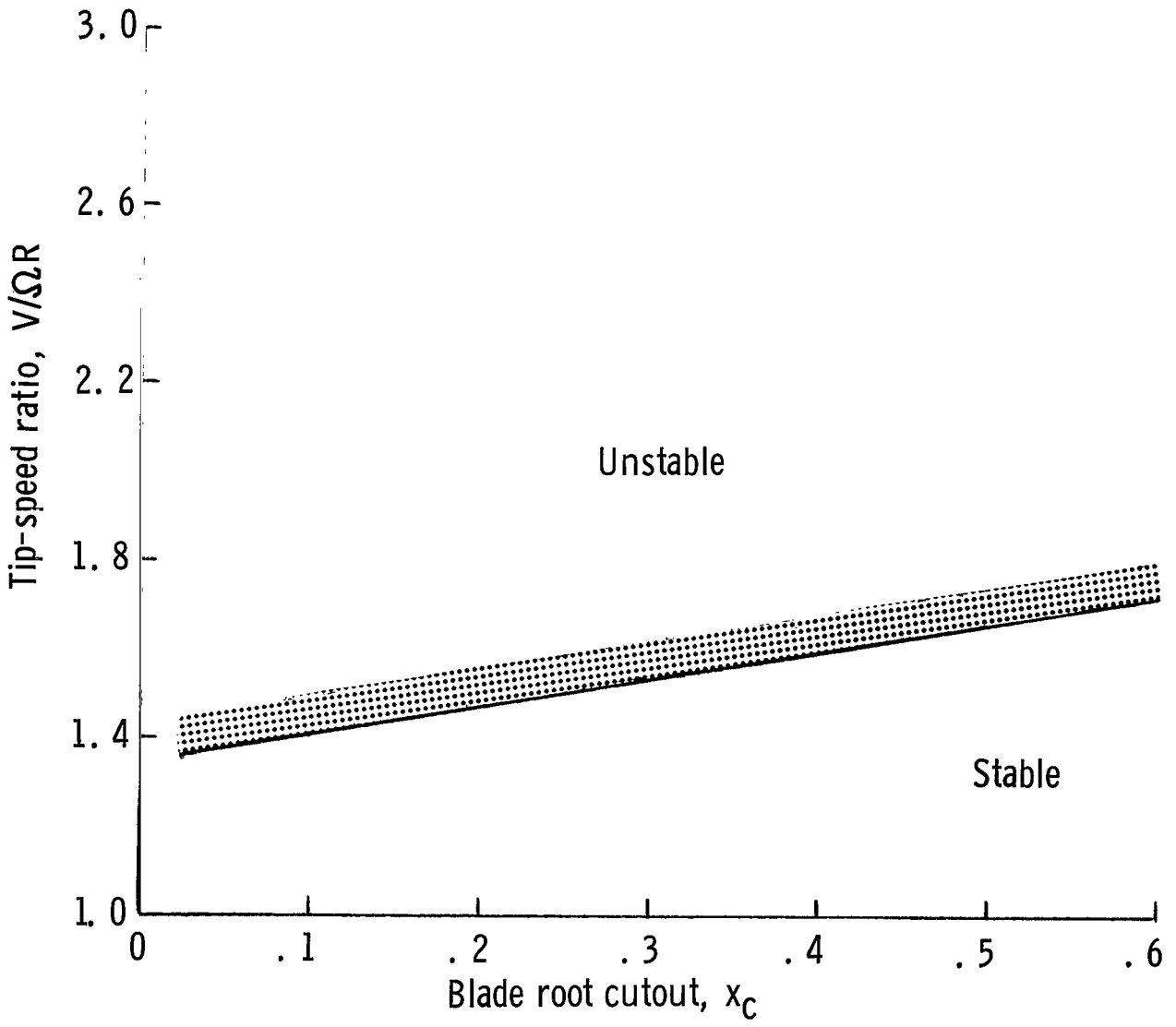

Figure 5.- Effect of blade-root cutout on blade-motion stability.

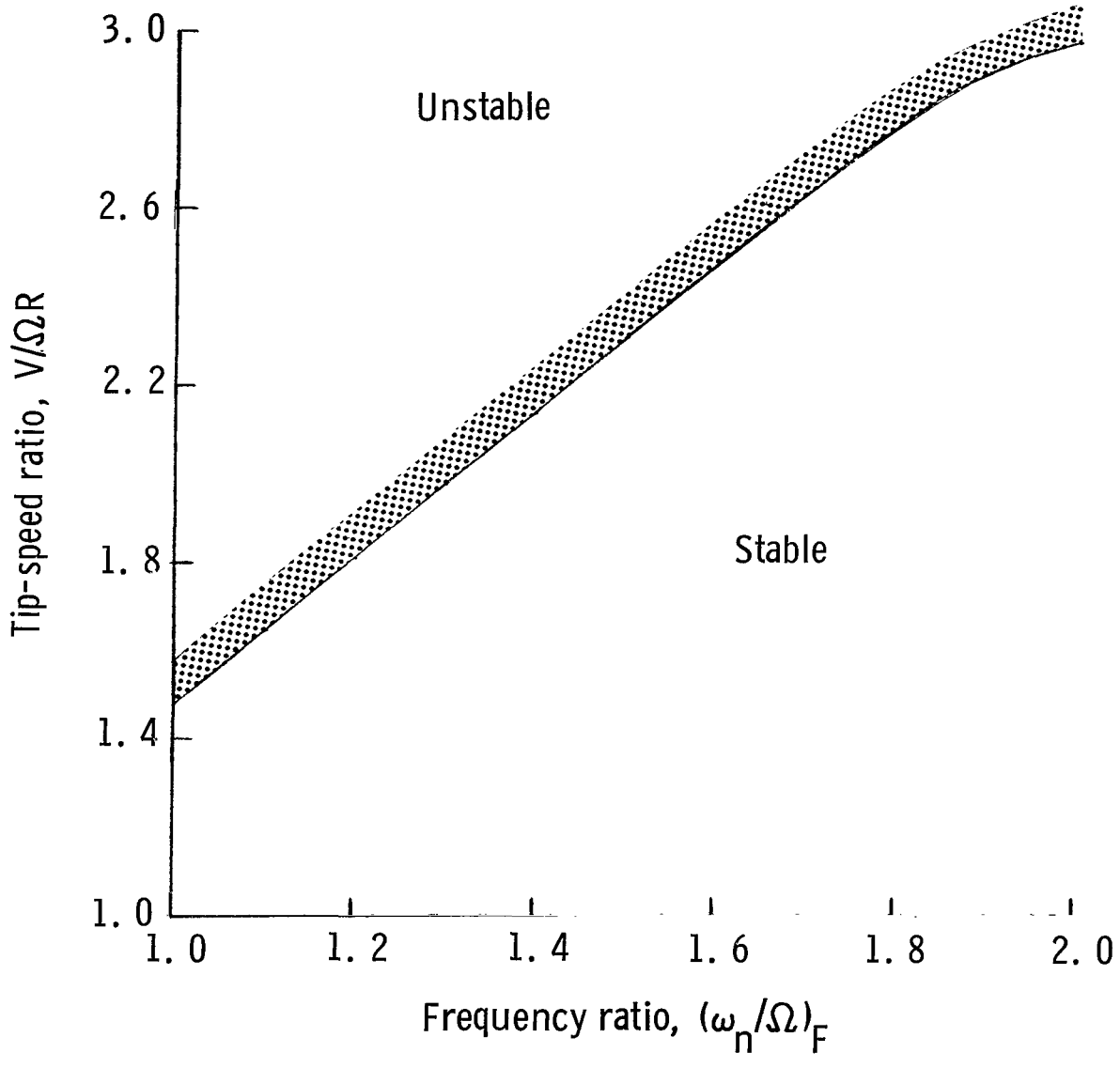

Figure 6.- Effect of flapping-hinge spring restraint on blade-motion stability.

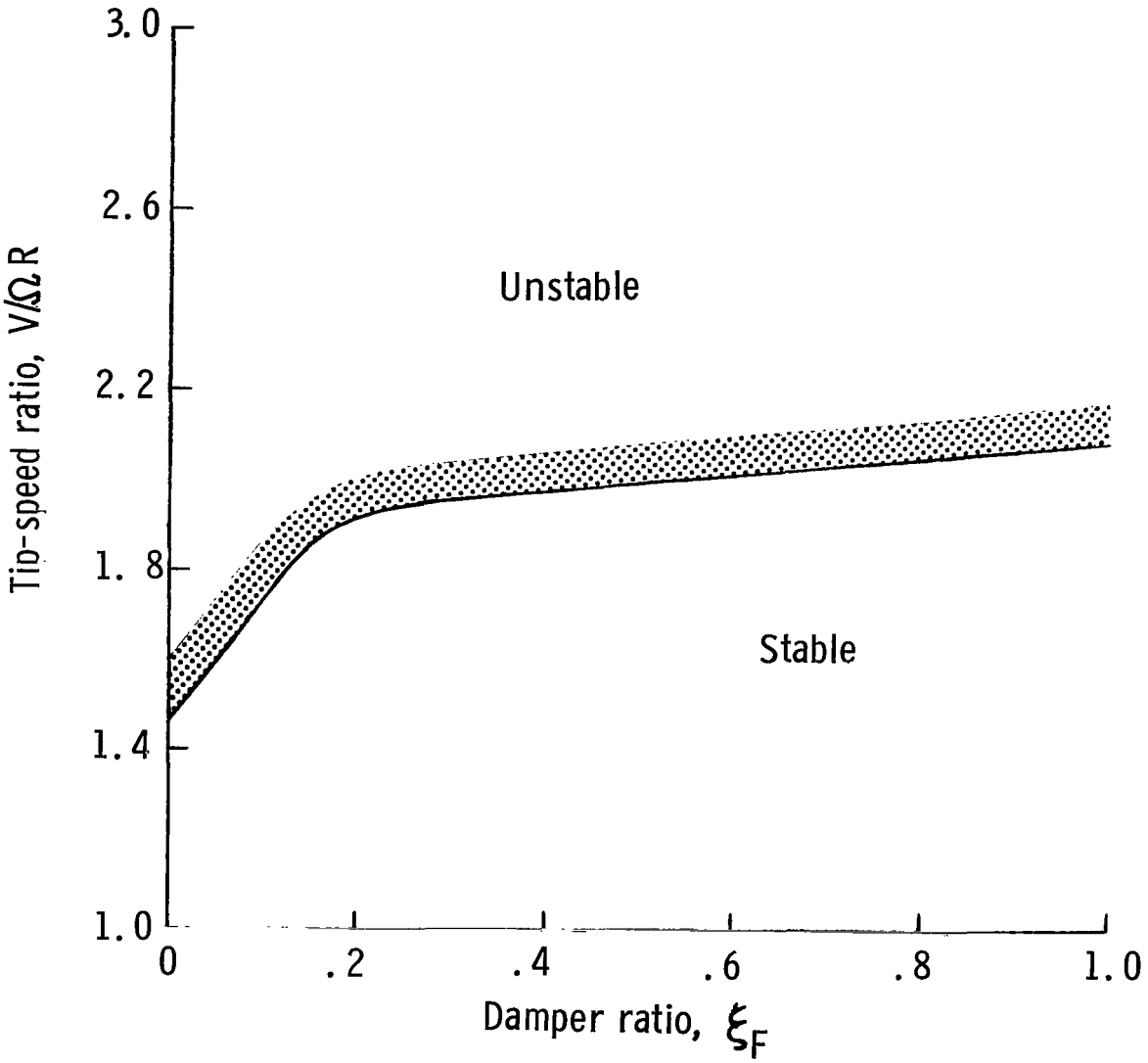

Figure 7.- Effect of flapping-hinge damping restraint on blade-motion stability.

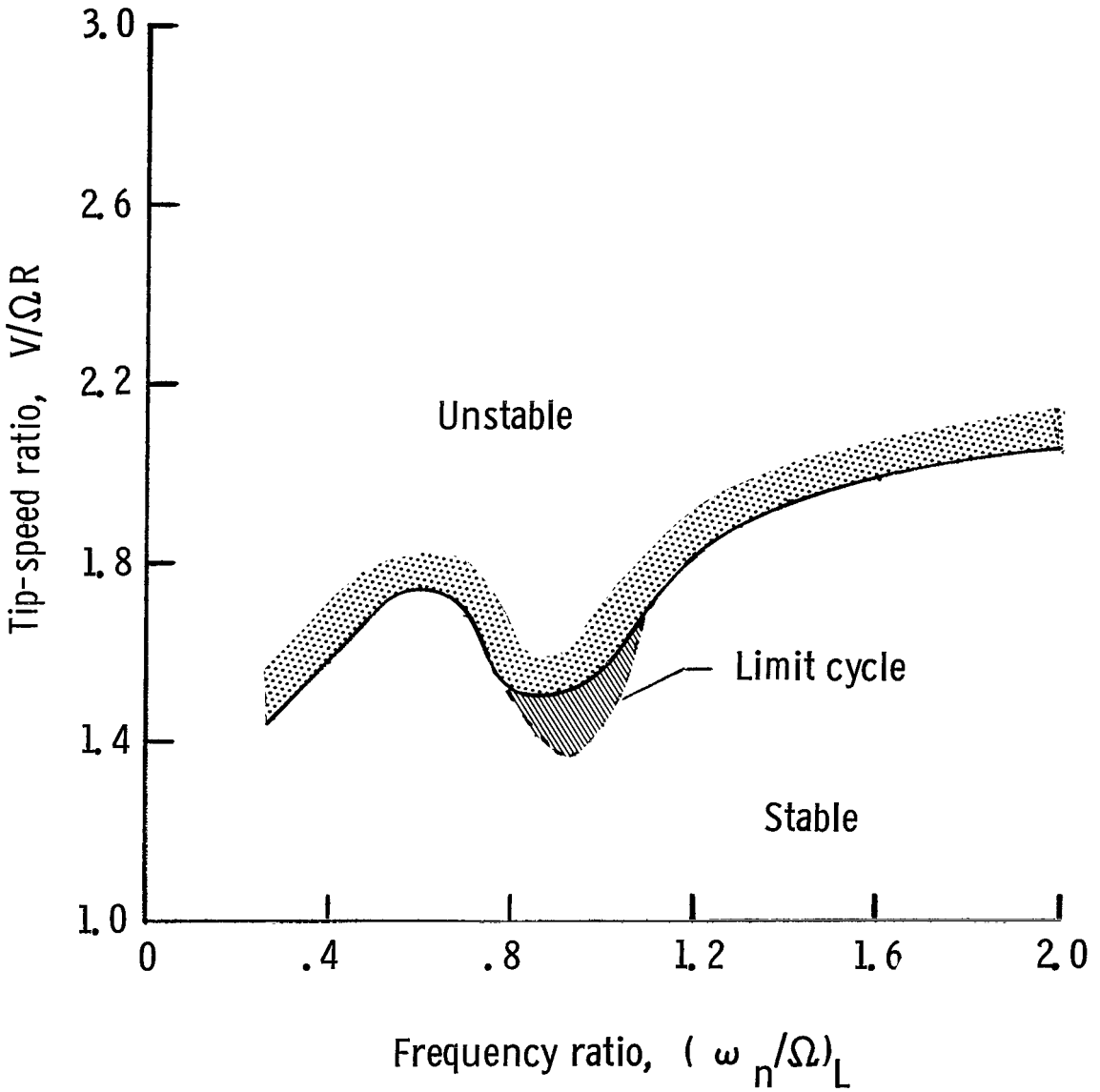

Figure 8.- Effect of lag-hinge spring restraint on blade-motion stability.

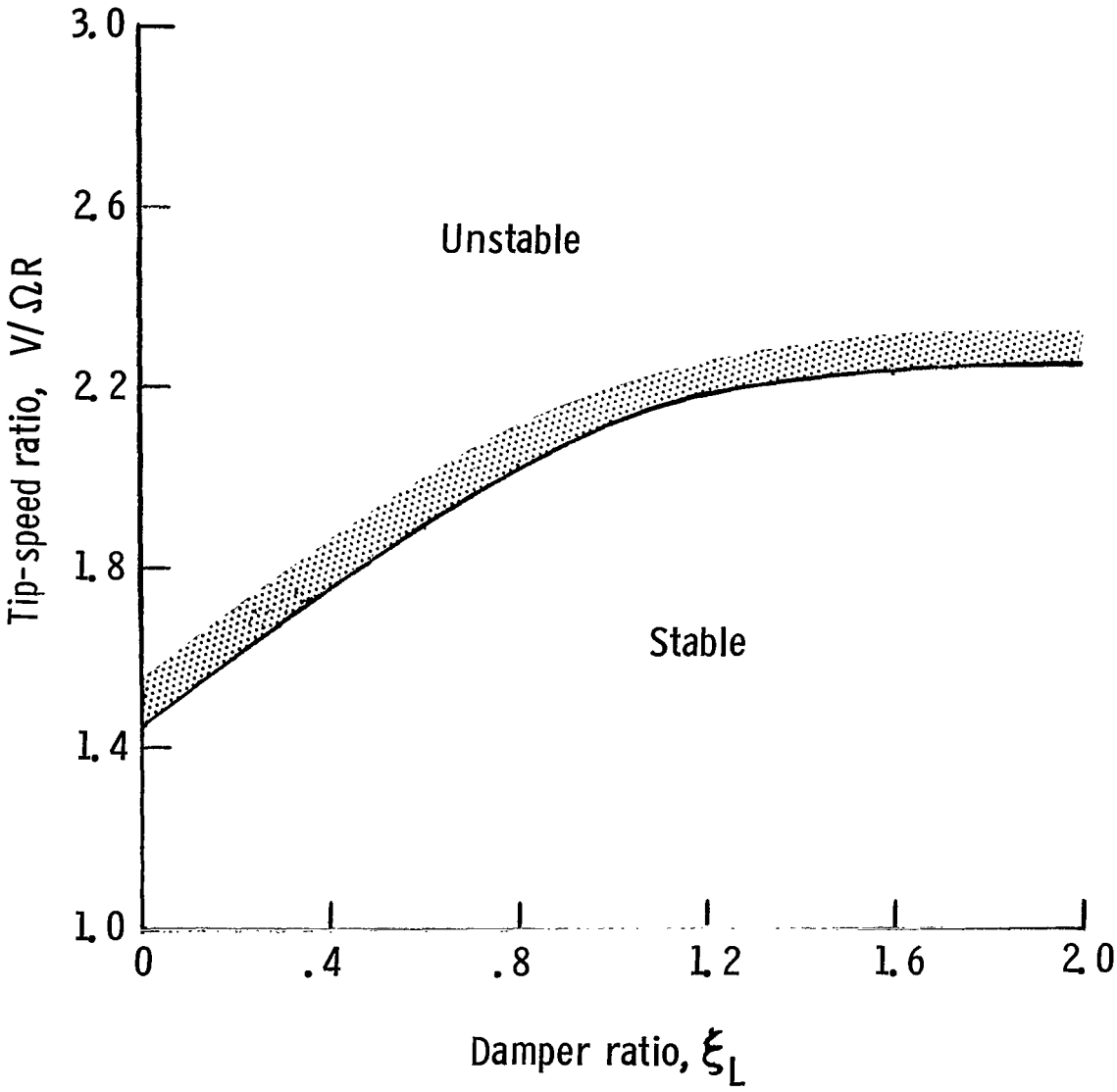

Figure 9.- Effect of lag-hinge damping restraint on blade-motion stability.

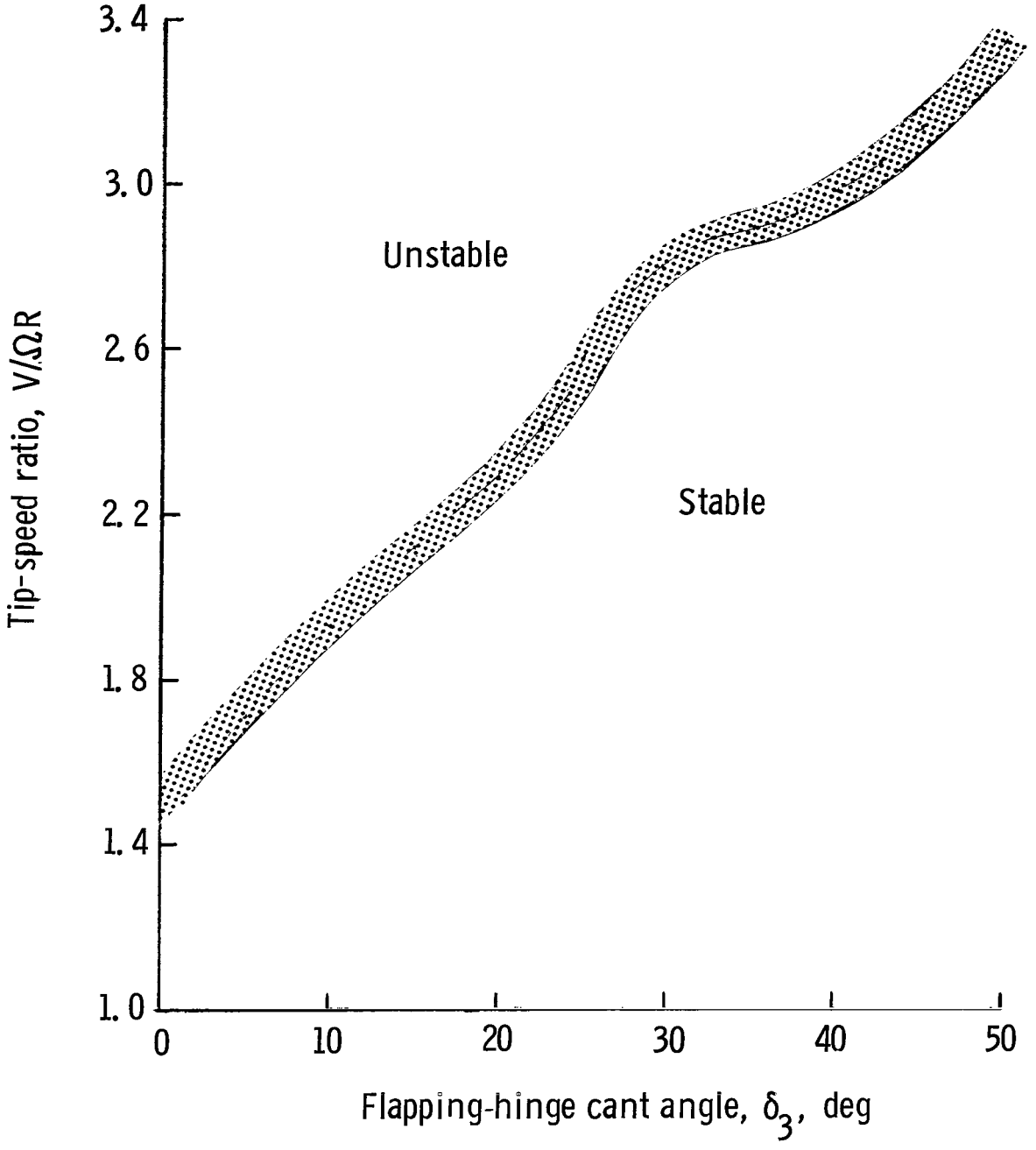

Figure 10.- Effect of flapping-hinge cant angle on blade-motion stability.

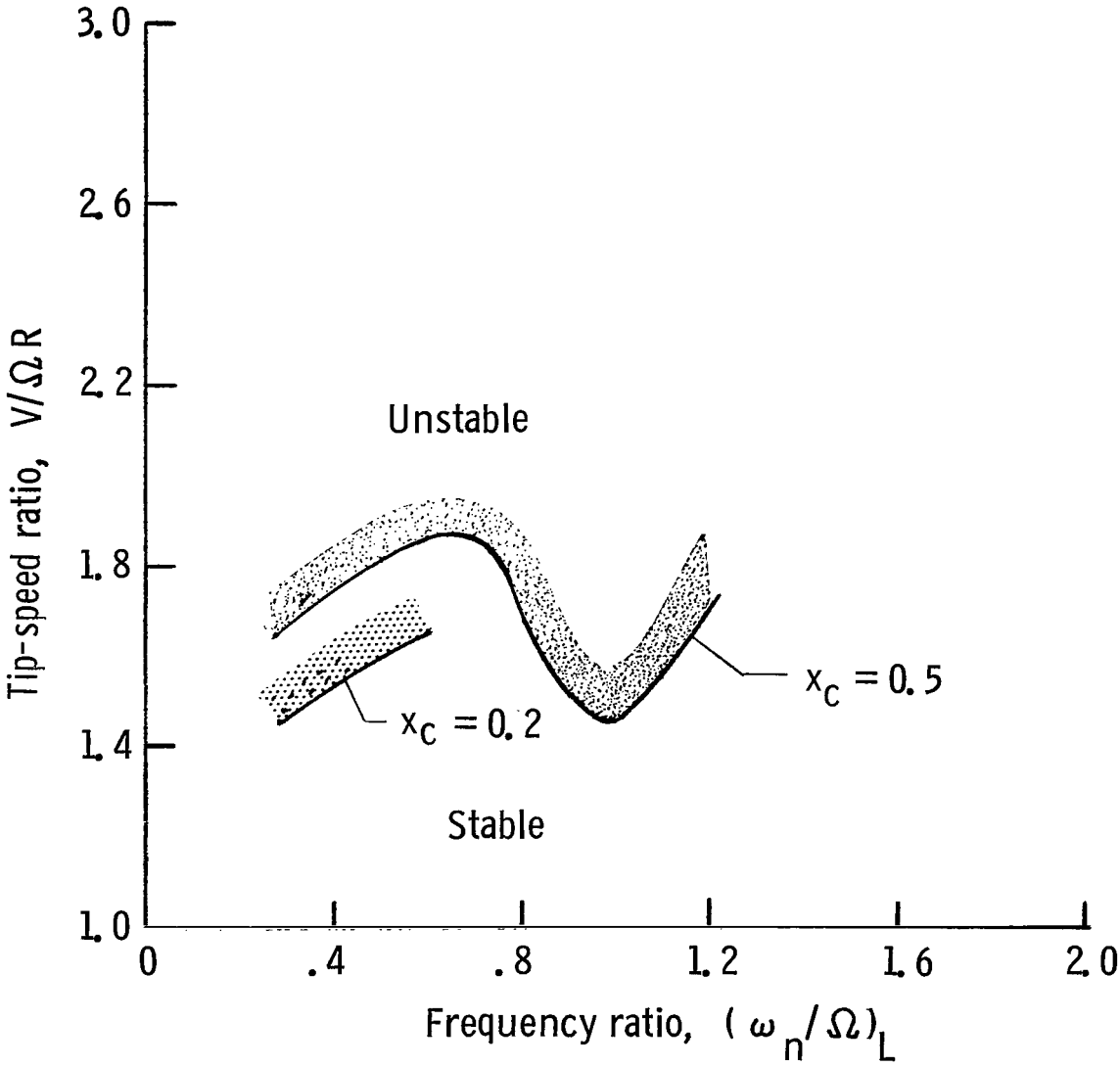

Figure 11.- Effect of lag-hinge offset on blade-motion stability.

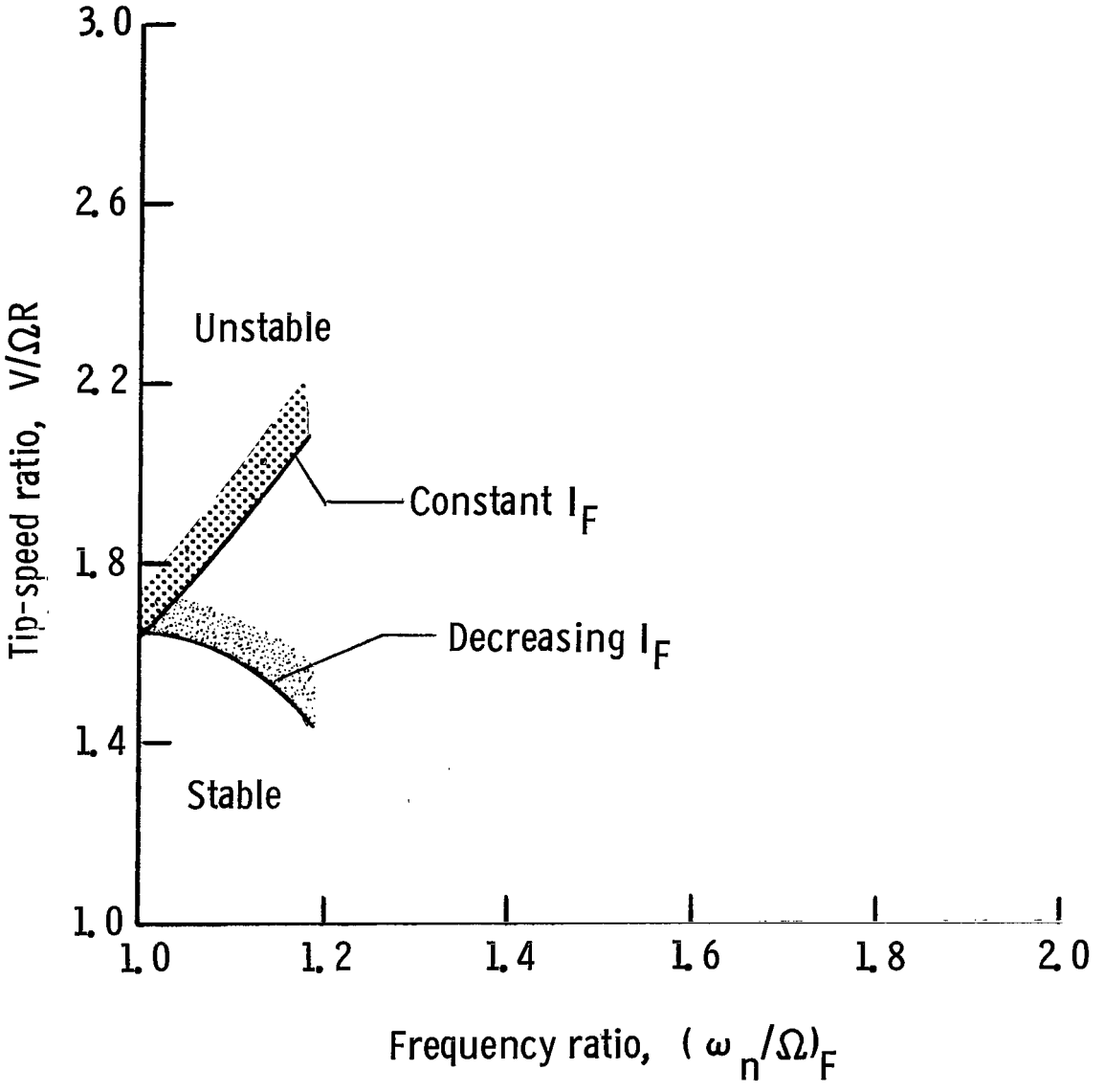

Figure 12.- Effect of flapping-hinge offset on blade-motion stability.

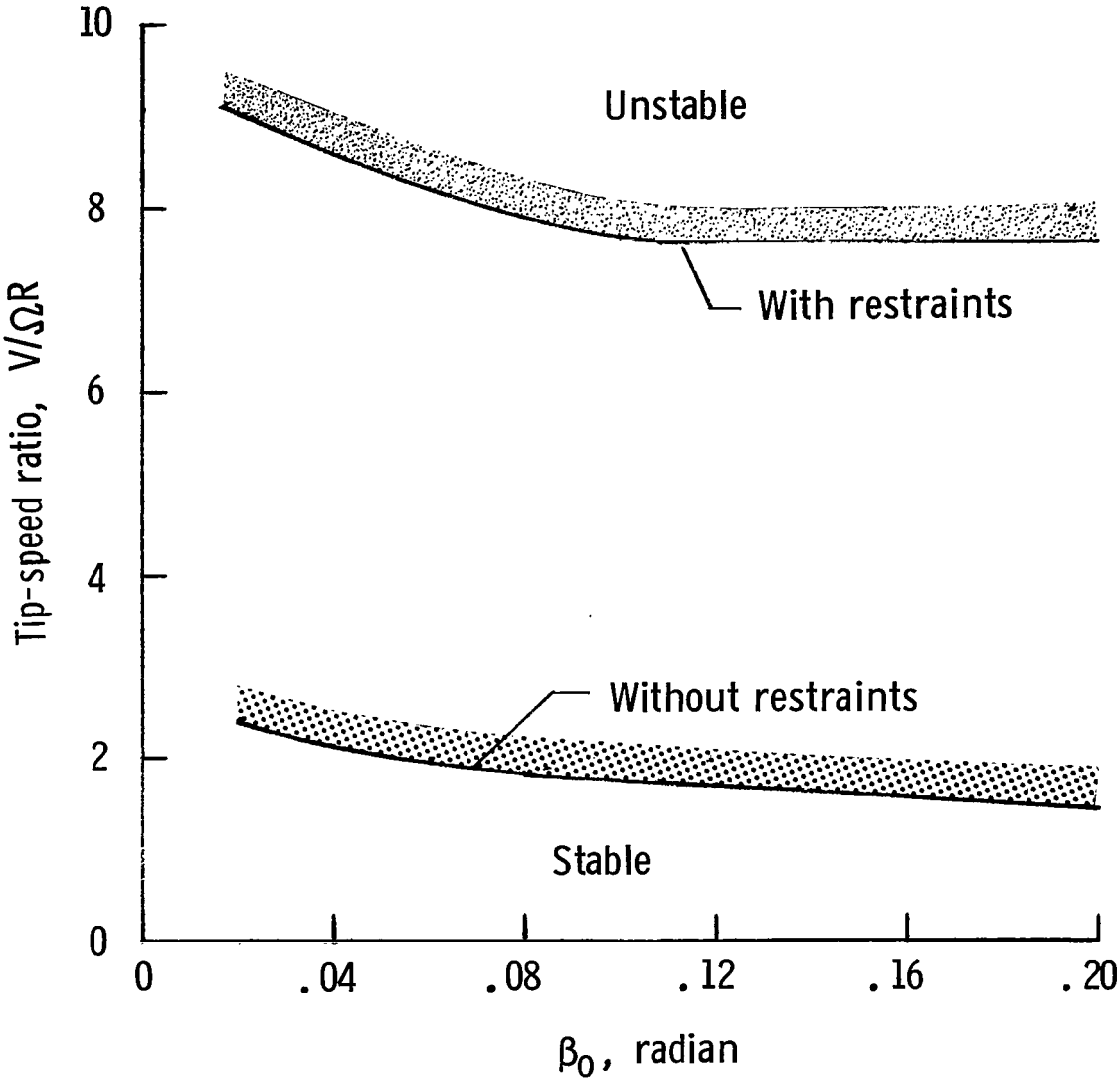

Figure 13.- Effect of combined restraints on blade-motion stability. $\psi_0 = 90^0$.

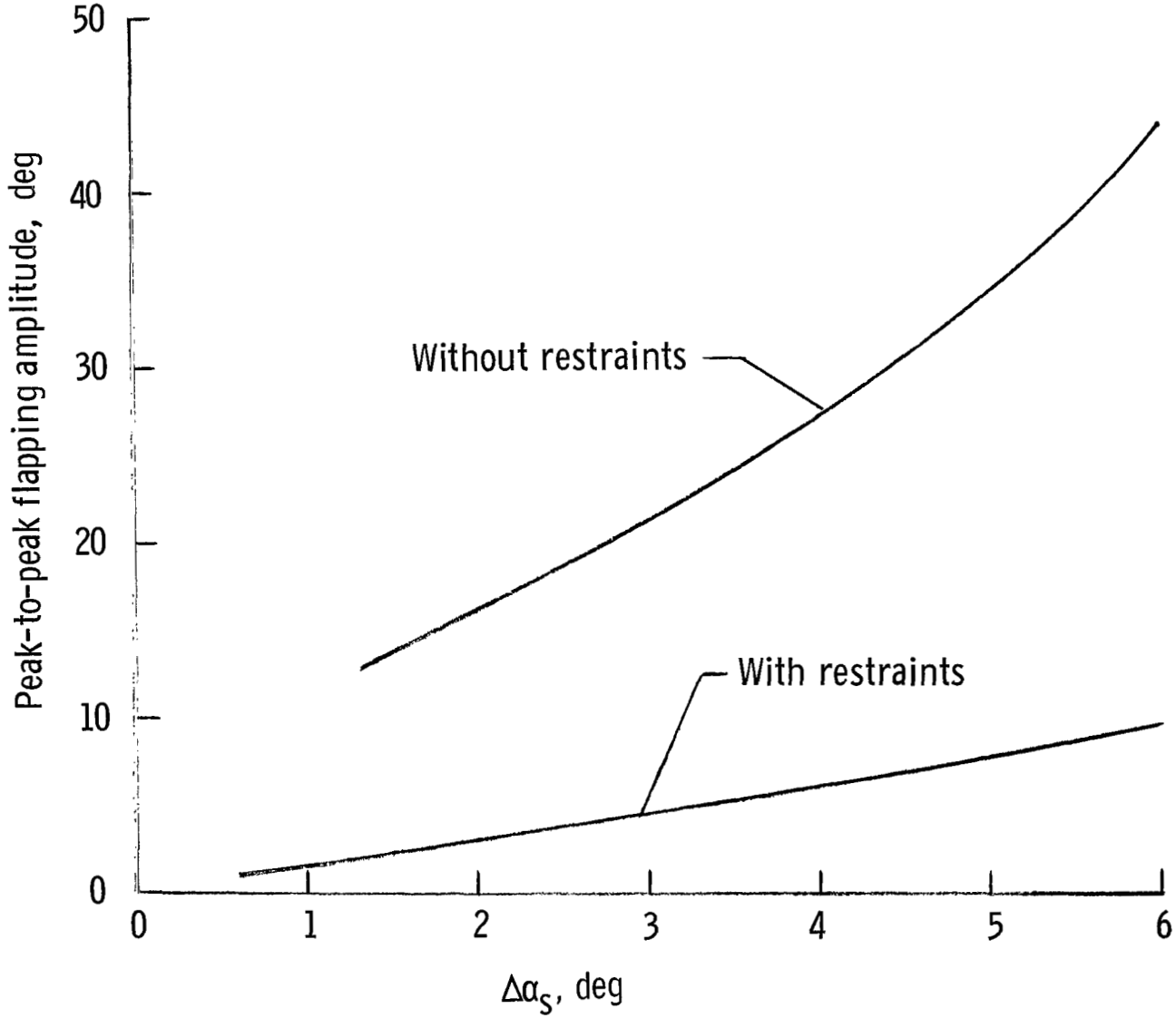

Figure 14.- Flapping-amplitude response to a shaft angle-of-attack step input. $V/\Omega R = 1.0$; $\psi_0 = 0^0$.

"The aeronautical and space activities of the United States shall be conducted so as to contribute . . . to the expansion of human knowledge of phenomena in the atmosphere and space. The Administration shall provide for the widest practicable and appropriate dissemination of information concerning its activities and the results thereof."

—NATIONAL AERONAUTICS AND SPACE ACT OF 1958

NASA SCIENTIFIC AND TECHNICAL PUBLICATIONS

TECHNICAL REPORTS: Scientific and technical information considered important, complete, and a lasting contribution to existing knowledge.

TECHNICAL NOTES: Information less broad in scope but nevertheless of importance as a contribution to existing knowledge.

TECHNICAL MEMORANDUMS: Information receiving limited distribution because of preliminary data, security classification, or other reasons.

CONTRACTOR REPORTS: Scientific and technical information generated under a NASA contract or grant and considered an important contribution to existing knowledge.

TECHNICAL TRANSLATIONS: Information published in a foreign language considered to merit NASA distribution in English.

SPECIAL PUBLICATIONS: Information derived from or of value to NASA activities. Publications include conference proceedings, monographs, data compilations, handbooks, sourcebooks, and special bibliographies.

TECHNOLOGY UTILIZATION PUBLICATIONS: Information on technology used by NASA that may be of particular interest in commercial and other non-aerospace applications. Publications include Tech Briefs, Technology Utilization Reports and Notes, and Technology Surveys.

Details on the availability of these publications may be obtained from:

SCIENTIFIC AND TECHNICAL INFORMATION DIVISION

NATIONAL AERONAUTICS AND SPACE ADMINISTRATION

Washington, D.C. 20546